Phys Chem Minerals (1982) 8:268–278

PHYSICS AND CHEMISTRY OF MINERALS
© Springer-Verlag 1982

Influence of Stacking Faults on the Spiral Growth of Polytype Structures in Mica

Dhananjai Pandey[1], A. Baronnet[2], and P. Krishna[3]

[1] School of Materials Science and Technology, Banaras Hindu University, Varanasi 221005, India
[2] Centre de Recherche sur les Mécanismes de la Croissance Cristalline, Campus de Luminy, Case 913, 13288 Marseille Cedex 09, France
[3] Department of Physics, Banaras Hindu University, Varanasi 221005, India

Abstract. A systematic theoretical deduction of polytype structures of mica that can result by the spiral growth mechanism operating in faulted $1M$, $2M_1$ and $3T$ basic matrices is reported. As a prerequisite, all possible intrinsic and extrinsic stacking fault configurations in each of the basic matrices have been worked out and their *stacking fault energy* (SFE) estimated. The deduction of polytype structures on the basis of the "faulted-matrix model" takes into account (i) the introduction of each of the low energy fault configurations in the exposed ledge of the screw dislocations, (ii) the change in the layer-position of the fault within the exposed ledge and (iii) the variation of the strength of the generating screw dislocation. At each stage, the spirally-grown polytypes are deduced for each basic structure. The most probable structures are predicted on the basis of the lowest SFE for the same strength of the screw dislocation and are then compared with the polytype structures reported in the literature. It was found that the faulted matrix model accounts successfully for the origin of all the polytype structures in mica. Furthermore, it may provide a basis for limiting the number of trial structures for determining the structures of long period polytypes.

Introduction

Polytypism in micas has received considerable attention during the last thirty years. The greatest part of this research has been devoted to the structural aspect of mica polytypism i.e., to the study of a structural control (Guven 1971) on the layer-stacking sequences connected with specific distortions in the structure of single layers. This concept has been developed by crystallographers on the basis of the refinement of over 30 structures of mica determined by X-ray, neutron and electron diffraction (for reviews see e.g. Bailey 1980; Baronnet 1980).

A considerable amount of experimental effort has also been directed towards the investigation of the phase aspect of mica polytypism. Owing to the specific distortions, although faint, of single layers involved in the common short-period stacking sequences (referred to by earlier workers as polymorphs), it has been believed that each of these could be stable phases within a given field of the $P_{H_2O}-T$ diagram, for a fixed chemical composition of the system. The ultimate goal of such a hypothesis was to use mica "polymorphs" as indicators of the intensive thermodynamic conditions prevailing during the genesis of mica-bearing rocks. Unfortunately, annealing experiments (Takeuchi and Haga 1971) on mica monocrystals to observe solid state structural transformations have failed to substantiate this hypothesis. On the basis of their experiments on the synthesis of mica, some workers (Yoder and Eugster 1954, 1955; Yoder 1959; Velde 1965a) have reported the following structural transformations as arising through crystallization from hydrothermal solution: $1\,Mrn(120) \rightarrow 1M$ and $2M_1 \rightarrow 1M$ for phlogopite, $1Mrn(120) \rightarrow 1M \rightarrow 2M_1$ and $3T \rightarrow 2M_1$ for muscovite[1]. These are very sluggish and are promoted by increasing temperature. From the monotropic character of these transformations and the tendency finally to attain a single form, the nature of which differs from species to species, it has been inferred that (i) there exists a unique stable stacking mode for a given mica viz. $1M$ for phlogopite and $2M_1$ for muscovite; (ii) the other modifications are metastable under steady state/equilibrium conditions and occur during mica synthesis because of growth kinetics effects like varying composition and/or supersaturation. Thus the $1Mrn(120) \rightarrow 1M \rightarrow 2M_1$ conversion sequence of muscovite observed at constant temperature should correspond to growth conditions under decreasing supersaturation (Baronnet 1980).

The growth aspect of mica polytypism was first envisaged by Amelinckx (1952) and Amelinckx and Dekeyser (1953) who postulated that a dislocation-free initial platelet of mica could develop only the disordered $1Mr$ structure and that ordered stacking sequences could originate only by the activity of growth spirals. Smith and Yoder (1956) suggested the possibility of structural control between the layers which would depend on the environmental conditions during the nucleation and layer by layer growth of the crystals. Depending on the strength of this structural control, the initial platelet formed during the nucleation and layer by layer growth period could adopt a perfectly ordered, more or less faulted or even completely disordered stacking sequence. It was suggested that the subsequent spiral

[1] $1Mrn(120)$ refers to a disordered sequence of the mica involving stacking of successive layers with $n \times 120°$ rotation between them, with n randomly chosen as 0, 1 or 2 along the sequence. In the one-layer monoclinic $1M$ structure, all single layers are stacked parallel to each other, whereas in the three-layer trigonal $3T$ structure, they are stacked with a constant $+120°$ rotation angle between consecutive layers. In the two-layer monoclinic structure $2M_1$, $+120°$ and $-120°$ rotation angles alternate regularly along the sequence.

0342-1791/82/0008/0268/$02.20

growth should play no role in the ordering of perfectly ordered mica "polymorphs" but only allow their growth under low supersaturation conditions. Screw dislocations could occasionally generate complex stacking sequences provided the initial platelet contained some growth faults. Smith and Yoder's proposal of "pre-ordering" during layer by layer growth has been supported by recent *transmission electron microscopy* (TEM) examination of the (001) face microtopography of synthetic mica crystallites, including OH-phlogopite (Baronnet 1972), OH-muscovite (Baronnet et al. 1976), paragonite and end members of the lepidolite group (Baronnet 1976). The pre-ordering in the initial platelet has been inferred from the step pattern of early first growth spirals on the micas, the exposed ledge structures of which often show a fully ordered sub-structure. In addition to the realization of Smith and Yoder's expectations, it was observed that growth spirals are also able to create new stacking sequences on a perfectly ordered parent platelet, if the pitch of the screw dislocation is a non-integral multiple of the repeat period of the parent matrix in accordance with Frank's (1951a) screw dislocation theory of polytypism.

A systematic theoretical deduction of all possible complex polytypes that could result from screw dislocations of non-integral Burgers vectors created in perfect $2M_1$, $2M_2$, $2O$ and $3T$ parent matrices has been carried out by Baronnet (1975). He has shown that of the seventeen complex polytypes known at that time, only seven could result from single screw dislocations operating in perfect parent matrices (perfect-matrix model). It was tentatively suggested that the growth of the remaining polytype structures should involve the occurrence of stacking faults or the coalescence of various basic structures within the exposed ledge of the generating screw dislocation. The present paper reports a systematic study of the influence of the stacking faults, present near the surface of the parent matrix at the time of the creation of the screw dislocation step, on the spiral growth of polytype structures in mica in accordance with the faulted matrix-model developed by Pandey and Krishna (1975a, b) for close-packed structures.

To describe the stacking sequences of mica layers, we shall use the conventional notations evolved by Ross et al. (1966) and by Zvyagin (1962) as detailed in the Appendix.

A preliminary report on the application of the faulted-matrix model to the genesis of mica polytypes has been published elsewhere (Baronnet et al. 1981).

The Faulted Matrix Model

A faulted matrix model for the spiral growth of polytype structures has recently been developed by Pandey and Krishna (1975a–d, 1976) to explain the origin of polytype structures in such materials as SiC, CdI_2 and PbI_2. The model considers the possibility that the parent matrix, formed during the nucleation and the layer by layer growth period, may be faulted and may contain low energy stacking faults near its surface at the time of the creation of the screw dislocation step. These faults may become incorporated into the structure of the screw dislocation step, which will then generate a polytype structure, even if it has an integral Burgers vector. The application of the faulted matrix model to a systematic deduction of polytype structures in mica can be achieved in the following steps:

(i) Postulate the different "basic structures" which are expected to be formed during the nucleation and the layer by layer growth;

(ii) Work out all possibly intrinsic and extrinsic stacking faults that are geometrically possible in each basic structure;

(iii) Estimate the *stacking fault energy* (SFE) of the various intrinsic and extrinsic fault configurations to determine the most probable fault configurations;

(iv) Deduce all possible polytype structures that can result from the winding of the screw dislocation step containing most probable fault configurations at different layer positions in the step;

(v) Estimate the SFE of the polytype structures so derived to predict the most probable series of polytype structures that can result from screw dislocations of equal strengths created in the same basic matrix containing the lowest energy fault configurations;

(vi) Compare the most probable series of structures predicted theoretically with those actually observed in micas.

The Basic Structures of Micas

The short period structures formed during nucleation and the layer by layer growth period will be considered as "basic structures" or "basic matrices" for the generation of complex polytype structures. As pointed out earlier, the basic structures may correspond either to a genuine thermodynamically stable phase (polymorphic phase) or a metastable phase formed because of growth-kinetic effects. It is believed that the basic structures for a given species of mica should actually correspond to the statistically most frequent short period structures in the natural as well as synthetic micas. Table 1 gives the relative frequency of occurrence of the various short period and the disordered $1Mrn(120)$ structures for various species of synthetic and natural micas. It is evident from the table that $1M$, $2M_1$ and $3T$ are the most common short period structures and will therefore be considered as "basic structures" for the generation of complex polytypes. This is justified in view of the fact that most of the complex polytype structures of mica contain one or more structure units of $1M$, $2M_1$ and $3T$ in their unit cells as evident from the last column of Table 1. Of the three other short period structures viz. $2M_2$, $2O$ and $6H$, originally envisaged by Smith and Yoder to result during the pre-ordering period, $6H$ has never been found while $2M_2$ is known to occur in lepidolites and $2O$ has been observed only very rarely. Also no complex polytype structure is known to be based on any of these three short period structures. We shall therefore not consider $2M_2$, $2O$ and $6H$, as basic structures. In addition, the disordered $1Mrn(120)$ structure cannot be retained in the deduction of polytype structures on the basis of the faulted matrix model since it is meaningless to introduce a stacking fault in it.

Stacking Faults in the Basic Structures of Mica

We shall extend the concept of intrinsic and extrinsic faults, first introduced by Frank (1951b) for close-packed structures, to classify the different possible fault configurations in the basic structures of mica. In the intrinsic type fault the perfect sequence of stacking vectors (Smith and Yoder 1956) extends right upto the fault plane whereas in the case of extrinsic faults the fault plane does not belong to

Table 1. Basic structures and polytypes in natural and synthetic micas

Species	Basic structures		Polytypes	
	Natural	Synthetic	Natural	Synthetic
Phlogopite	$1M>2M_1$, $3T$, $1Mrn(120)$ [i]	$1M$, $1Mrn(120)$ [i]		$4Tc[0132]$ [xxx] *
Siderophyllite	$1M$, $2M_1$ [ii]	$1M$ [iii]	$3Tc[02\bar{2}]$ [iv], $9Tc[(0_7 2\bar{2}]$ [ii]	–
Biotites	$1M>2M_1>3T$ [iv, v, xxix]	$1M>>2M_1$ [iv, vi, vii]	$4Tc[(0)_2 2\bar{2})$, $8Tc[(0)_6 2\bar{2})$, $14Tc[(0)_{12} 2\bar{2}]$	–
			$23Tc[(0)_{21} 2\bar{2}]$, $8Tc[(2\bar{2})_3 \bar{2}2]$, $4M[2220]$	–
			$8M[(222)_2 2\bar{2}]$, $11M[(222)_3 2\bar{2}]$, $8Tc[(0)_7 2\bar{2}]$, $10Tc[(2)_5 \bar{2}2200]$ [iv]	
Zinnwaldites	$1M>2M_1$, $3T$ [ii, xxix]	$1M$ [iii]	$9Tc[(0)_7 2\bar{2}]$, $5M[22222\bar{2})$, $14M[222)_4 2\bar{2}]$ [ii]	–
Lepidolites	$1M$, $2M_2>3T>>2M_1$ [ix, xi, xxix]	$1M$, $2M_1$, $2M_2$? [viii]	$3M[11\bar{2}]$ [xxxi]	–
Clintonite	$1M$, $2M_1$ [v]	$1M$, $1Mrn(120)$ [xii]	–	–
Muscovite	$2M_1>>3T$, $1M$, $1Mrn(120)$ [xiii, xxix]	$2M_1$, $1M$, $1Mrn(120)$ [xiii, xiv]	–	$3Tc[02\bar{2}]$, $5Tc[0(2\bar{2})_2]$ [xxviii]
Phengite	$2M_1$, $3T>1M$ [xv–xx] $>>2M_2$ [xxxiii]	$2M_1$, $1M$ [xxi, xxii]	–	$3Tc[02\bar{2}]$ [xxxii]
Paragonite	$2M_1$ [xxiii]	$2M_1$, $1Mrn(120)$ [xxiv, xxv]	–	$3Tc[02\bar{2}]$ [xxxii]
Margarite	$2M_1$ [v]	$2M$, $1Mrn(120)$ [xxvi, xxvii]	–	–

[i] Yoder and Eugster 1954, [ii] Rieder 1970, [iii] Rieder 1971, [iv] Ross et al. 1966, [v] Deer et al. 1965, [vi] Wones 1963, [vii] Hewitt and Wones 1975, [viii] Munoz 1968, [ix] Foster 1960, [x] Levinson 1953, [xi] Cerny et al. 1970, [xii] Olesch 1975, [xiii] Yoder and Eugster 1955, [xiv] Velde 1965a, [xv] Ernst 1963, [xvi] Beugnies et al. 1969, [xvii] Fiorentini Potenza and Morelli 1968, [xviii] Blasi and Blasi de Pol 1973, [xix] Dunoyer de Segonzac and Hickel 1972, [xx] Velde 1970, [xxi] Crowley and Roy 1964, [xxii] Velde 1965b, [xxiii] Harder 1956, [xxiv] Eugster and Yoder 1954, [xxv] Chatterjee 1970, [xxvi] Velde 1971, [xxvii] Chatterjee 1971, [xxviii] Baronnet et al. 1976, [xxix] Koval' et al. 1975, [xxx] Takeda 1967, [xxxi] Bailey and Christie 1978, [xxxii] Baronnet 1980, [xxxiii] Zhoukhlistov et al. 1973

* Synthetic Li-fluorphlogopite
(Modified from Baronnet 1980)

Table 2. List of possible fault configurations in $1M[0]$ structure and their *stacking fault energy* (SFE)

S.No.	Fault	Zvyagin symbol	RTW symbol	SFE
1.	I_0^1	$\ldots CCCC \vdots \bar{B}\bar{B}\bar{B}\bar{B}\ldots$	$\ldots(0)_p 1(0)_q\ldots$	$\phi_1(1)+2\phi_2$
2.	I_0^2	$\ldots CCCC \vdots AAAA\ldots$	$\ldots(0)_p 2(0)_q\ldots$	$\phi_1(2)+2\phi_2$
3.	I_0^3	$\ldots CCCC \vdots \bar{C}\bar{C}\bar{C}\bar{C}\ldots$	$\ldots(0)_p 3(0)_q\ldots$	$\phi_1(3)+2\phi_2$
4.	$E_0^{1\bar{1}}$	$\ldots CCCC \vdots \bar{A} \vdots CCCC\ldots$	$\ldots(0)_p\bar{1}1(0)_q\ldots$	$2\phi_1(1)+3\phi_2$
5.	$E_0^{\bar{2}2}$	$\ldots CCCC \vdots A \vdots CCCC\ldots$	$\ldots(0)_p\bar{2}2(0)_q\ldots$	$2\phi_1(2)+3\phi_2$
6.	E_0^{33}	$\ldots CCCC \vdots \bar{C} \vdots CCCC\ldots$	$\ldots(0)_p 33(0)_q\ldots$	$2\phi_1(3)+3\phi_2$

Note: Dotted vertical line indicates the fault plane with respect to the perfect stacking sequence on its left hand side

the perfect stacking sequence on either side of it. The method used here for deducing the possible fault configurations is based on the method suggested by Pandey and Krishna (1975d, 1976) for close-packed structures. We shall use the standard Zvyagin notation for deducing the fault configurations and the Ross-Takeda-Wones (RTW) symbols for providing a compact notation to represent them (cf. also Appendix). It it found that the fault configurations in the basic structures of mica can be completely specified by symbols like $I_p^{qrs\cdots}$ or $E_p^{qrs\cdots}$ where I and E stand for *intrinsic* and *extrinsic* respectively, $qrs\ldots$ for the RTW symbols not forming a part of the regular RTW sequence and p for the RTW symbol just preceding the first faulted RTW symbol (q). It is easy to see that fault configurations $I_p^{qrs\cdots}$

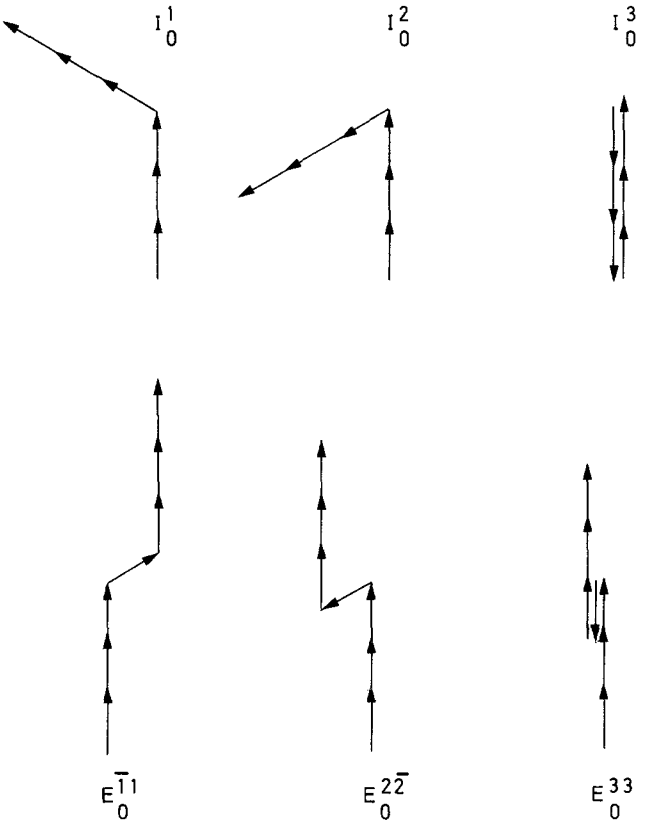

Fig. 1. Irreducible types of intrinsic and extrinsic fault configurations in the $1M$ basic matrix

and $E_p^{qrs\cdots}$ are enantiomorphous with $I_{\bar{p}}^{\bar{q}\bar{r}\bar{s}\cdots}$ and $E_{\bar{p}}^{\bar{q}\bar{r}\bar{s}\cdots}$, respectively. Most of the intrinsic fault configurations correspond to twin configurations in the conventional sense.

Possible Fault Configurations in the 1M[O] Structure

The $1M$[0] structure can be written as $\ldots CCC\ldots$ in the Zvyagin notation. During the layer by layer growth of a crystal with the $\ldots CCCC\ldots$ stacking sequence, a fresh $1M$[0] sequence can start in five different ways corresponding to the five different orientations which the first faulted layer can adopt. These are, $\ldots AAAA\ldots$, $\bar{A}\bar{A}\bar{A}\bar{A}\ldots$, $BBBB\ldots$, $\ldots\bar{B}\bar{B}\bar{B}\bar{B}\ldots$ and $\ldots\bar{C}\bar{C}\bar{C}\bar{C}\ldots$. This leads to five possible intrinsic fault configurations. Of these, $I_0^{\bar{1}}$ and $I_0^{\bar{2}}$ are enantiomorphous with I_0^1 and I_0^2 respectively leaving only three unique intrinsic fault configurations in the $1M$ [0] structure as depicted in Fig. 1. The intrinsic faults in $1M$[0] actually correspond to twin configurations. These are listed in Table 2 in Zvyagin, RTW and $I_p^{qrs\cdots}$ notations. I_0^2 and I_0^3 were considered by Smith and Yoder (1956) as common twinning modes in natural $1M$ micas. The extrinsic fault configurations were deduced by inserting A, $\bar{A}$, B, $\bar{B}$ and $\bar{C}$ type layers in the $\ldots CCCC\ldots$ sequence. This provides us only three unique extrinsic fault configurations in the $1M$[0] structure which are also listed in Table 2 and represented by their stacking vectors in Fig. 1.

Possible Fault Configurations in the $2M_1[2\bar{2}]$ Structure

In the $2M_1[2\bar{2}]$ or $\ldots\bar{A}\bar{B}\bar{A}\bar{B}\ldots$ structure, an intrinsic fault configuration can commence at any of the two layer positions in the two-layer monoclinic unit cell. If the intrinsic fault commences after $\bar{B}$ type layer, then the first faulted layer can be A, B, $\bar{B}$, C or $\bar{C}$. Corresponding to each of these five possibilities, there are two different ways in which the subsequent $2M_1$ sequence may follow. This provides ten possible intrinsic fault configurations that can occur after the $\bar{B}$ type layer in the $\bar{A}\bar{B}$ unit cell. Similarly one can obtain another ten fault configurations after $\bar{A}$ type

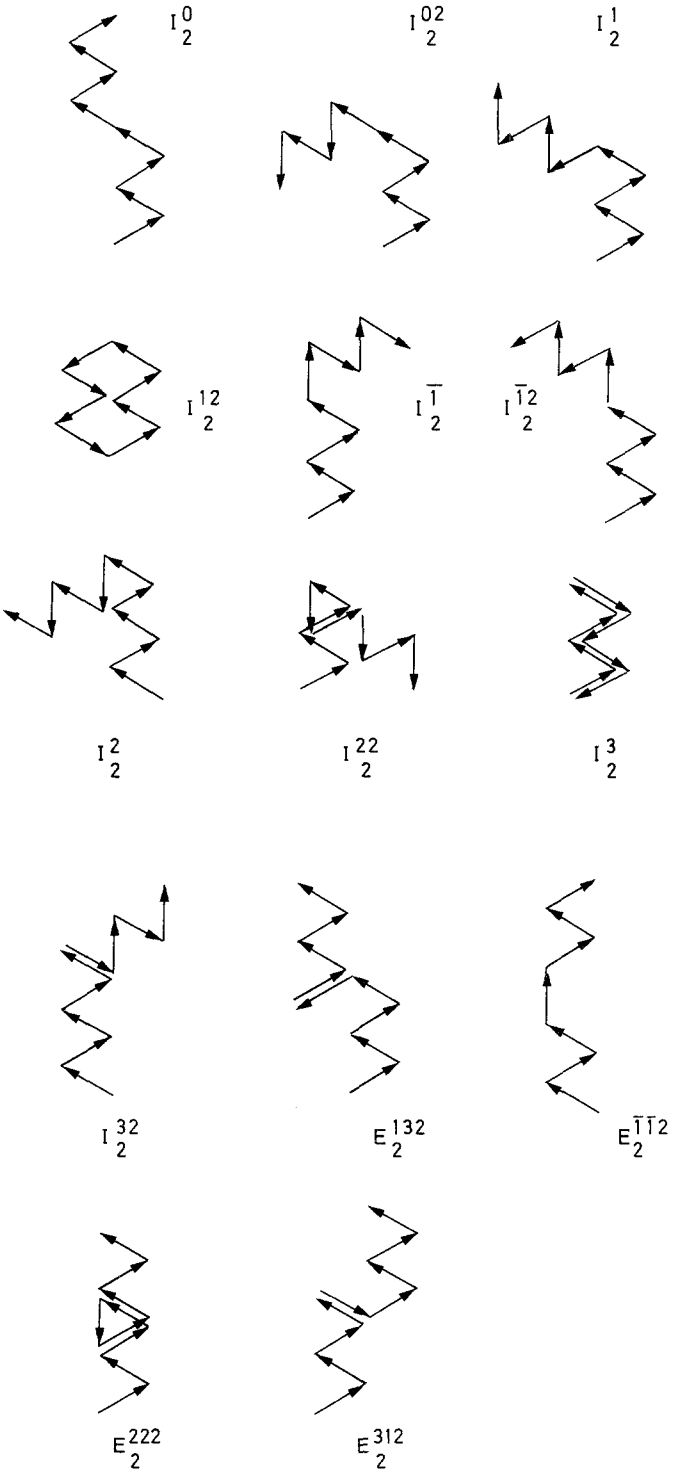

Fig. 2. Irreducible types of intrinsic and extrinsic fault configurations in the $2M_1$ basic matrix

Table 3. List of possible fault configurations in $2M_1[2\bar{2}]$ structure and their *stacking fault energy* (SFE)

S.No.	Fault type	Zvyagin symbol	RTW symbol	SFE
1.	I_2^0	$\ldots\bar{A}\bar{B}\bar{A}\bar{B}\,\vdots\,\bar{B}\bar{A}\bar{B}\bar{A}\ldots$	$\ldots(\bar{2}2)_p0(\bar{2}2)_q\ldots$	$\phi_1(0)+2\phi_2$
2.	I_2^{02}	$\ldots\bar{A}\bar{B}\bar{A}\bar{B}\,\vdots\,\bar{B}\bar{C}\bar{B}\bar{C}\ldots$	$\ldots(\bar{2}2)_p02(\bar{2}2)_q\ldots$	$\phi_1(0)+2\phi_2$
3	I_2^1	$\ldots\bar{A}\bar{B}\bar{A}\bar{B}\,\vdots\,ACAC\ldots$	$\ldots(\bar{2}2)_p1(\bar{2}2)_q\ldots$	$\phi_1(1)+2\phi_2$
4.	I_2^{12}	$\ldots\bar{A}\bar{B}\bar{A}\bar{B}\,\vdots\,ABAB\ldots$	$\ldots(\bar{2}2)_p12(\bar{2}2)_q\ldots$	$\phi_1(1)+2\phi_2$
5.	$I_2^{\bar{1}}$	$\ldots\bar{A}\bar{B}\bar{A}\bar{B}\,\vdots\,CBCB\ldots$	$\ldots(\bar{2}2)_p\bar{1}(\bar{2}2)_q\ldots$	$\phi_1(1)+2\phi_2$
6.	$I_2^{\bar{1}2}$	$\ldots\bar{A}\bar{B}\bar{A}\bar{B}\,\vdots\,CACA\ldots$	$\ldots(\bar{2}2)_p\bar{1}2(\bar{2}2)_q\ldots$	$\phi_1(1)+2\phi_2$
7.	I_2^2	$\ldots\bar{A}\bar{B}\bar{A}\bar{B}\,\vdots\,\bar{C}\bar{B}\bar{C}\bar{B}\ldots$	$\ldots(\bar{2}2)_p2(\bar{2}2)_q\ldots$	$0\phi_1+\phi_2$
8.	I_2^{22}	$\ldots\bar{A}\bar{B}\bar{A}\bar{B}\,\vdots\,\bar{C}\bar{A}\bar{C}\bar{A}\ldots$	$\ldots(\bar{2}2)_p22(\bar{2}2)_q\ldots$	$0\phi_1+2\phi_2$
9.	I_2^3	$\ldots\bar{A}\bar{B}\bar{A}\bar{B}\,\vdots\,BABA\ldots$	$\ldots(\bar{2}2)_p3(\bar{2}2)_q\ldots$	$\phi_1(3)+2\phi_2$
10.	I_2^{32}	$\ldots\bar{A}\bar{B}\bar{A}\bar{B}\,\vdots\,BCBC\ldots$	$\ldots(\bar{2}2)_p32(\bar{2}2)_q\ldots$	$\phi_1(3)+2\phi_2$
11.	E_2^{132}	$\ldots\bar{A}\bar{B}\bar{A}\bar{B}\,\vdots\,A\,\vdots\,\bar{A}\bar{B}\bar{A}\bar{B}\ldots$	$\ldots(\bar{2}2)_p132(\bar{2}2)_q\ldots$	$\phi_1(1)+\phi_1(3)+3\phi_2$
12.	$E_2^{\bar{1}\bar{1}2}$	$\ldots\bar{A}\bar{B}\bar{A}\bar{B}\,\vdots\,C\,\vdots\,\bar{A}\bar{B}\bar{A}\bar{B}\ldots$	$\ldots(\bar{2}2)_p\bar{1}\bar{1}2(\bar{2}2)_q\ldots$	$2\phi_1(1)+3\phi_2$
13.	E_2^{222}	$\ldots\bar{A}\bar{B}\bar{A}\bar{B}\,\vdots\,C\,\vdots\,\bar{A}\bar{B}\bar{A}\bar{B}\ldots$	$\ldots(\bar{2}2)_p222(\bar{2}2)_q\ldots$	$0\phi_1+3\phi_2$
14.	E_2^{312}	$\ldots\bar{A}\bar{B}\bar{A}\bar{B}\,\vdots\,B\,\vdots\,\bar{A}\bar{B}\bar{A}\bar{B}\ldots$	$\ldots(\bar{2}2)_p312(\bar{2}2)_q\ldots$	$\phi_1(1)+\phi_1(3)+3\phi_2$

Note: Dotted vertical line indicates the fault plane with respect to the perfect stacking sequence on its left hand site

Table 4. List of possible fault configurations in the $3T[222]$ structure and their stacking fault energy

S.No.	Fault type	Zvyagin symbol	RTW symbol	SFE
1.	I_t^0	$\ldots ABCABC\,\vdots\,CABCAB\ldots$	$(222)_p0(222)_q$	$\phi_1(0)+2\phi_2$
2.	$I_{t'}^0$	$\ldots ABCABC\,\vdots\,CBACBA\ldots$	$(222)_p0(\bar{2}\bar{2}\bar{2})_q$	$\phi_1(0)+2\phi_2$
3.	I_t^1	$\ldots ABCABC\,\vdots\,\bar{B}\bar{C}\bar{A}\bar{B}\bar{C}\bar{A}\ldots$	$(222)_p1(222)_q$	$\phi_1(1)+2\phi_2$
4.	$I_{t'}^1$	$\ldots ABCABC\,\vdots\,\bar{B}\bar{A}\bar{C}\bar{B}\bar{A}\bar{C}\ldots$	$(222)_p1(\bar{2}\bar{2}\bar{2})_q$	$\phi_1(1)+2\phi_2$
5.	$I_t^{\bar{1}}$	$\ldots ABCABC\,\vdots\,\bar{A}\bar{B}\bar{C}\bar{A}\bar{B}\bar{C}\ldots$	$(222)_p\bar{1}(222)_q$	$\phi_1(1)+2\phi_2$
6.	$I_{t'}^{\bar{1}}$	$\ldots ABCABC\,\vdots\,\bar{A}\bar{C}\bar{B}\bar{A}\bar{C}\bar{B}\ldots$	$(222)_p\bar{1}(\bar{2}\bar{2}\bar{2})_q$	$\phi_1(1)+2\phi_2$
7.	$I_t^{\bar{2}}$	$\ldots ABCABC\,\vdots\,BCABCA\ldots$	$(222)_p\bar{2}(222)_q$	$0\phi_1+2\phi_2$
8.	$I_{t'}^{\bar{2}}$	$\ldots ABCABC\,\vdots\,BACBAC\ldots$	$(222)_p(\bar{2}\bar{2}\bar{2})_q$	$0\phi_1+\phi_2$
9.	I_t^3	$\ldots ABCABC\,\vdots\,\bar{C}\bar{A}\bar{B}\bar{C}\bar{A}\bar{B}\ldots$	$(222)_p3(222)_q$	$\phi_1(3)+2\phi_2$
10.	$I_{t'}^3$	$\ldots ABCABC\,\vdots\,\bar{C}\bar{B}\bar{A}\bar{C}\bar{B}\bar{A}\ldots$	$(222)_p3(\bar{2}\bar{2}\bar{2})_q$	$\phi_1(3)+2\phi_2$
11.	E_t^{11}	$\ldots ABCABC\,\vdots\,\bar{B}\,\vdots\,ABCABC\ldots$	$(222)_p11(222)_q$	$2\phi_1(1)+3\phi_2$
12.	$E_t^{\bar{2}\bar{2}}$	$\ldots ABCABC\,\vdots\,B\,\vdots\,ABCABC\ldots$	$(222)_p\bar{2}\bar{2}(222)_q$	$0\phi_1+2\phi_2$
13.	$E_t^{\bar{1}3}$	$\ldots ABCABC\,\vdots\,\bar{A}\,\vdots\,ABCABC\ldots$	$(222)_p\bar{1}3(222)_q$	$\phi_1(1)+\phi_1(3)+3\phi_2$
14.	$E_t^{3\bar{1}}$	$\ldots ABCABC\,\vdots\,\bar{C}\,\vdots\,ABCABC\ldots$	$(222)_p3\bar{1}(222)_q$	$\phi_1(1)+\phi_1(3)+3\phi_2$

Note: Dotted vertical line indicates the fault plane with respect to the perfect stacking sequence on its left hand side

layer. By drawing the linked stacking vectors for all these fault configurations, it can be shown that the intrinsic fault configurations occurring after the $\bar{B}$ type layer are enantiomorphous with those occuring after the $\bar{A}$ type layer. Thus we are left with only ten unique intrinsic fault configurations in the $2M_1$ structure.

The extrinsic fault configurations were deduced by inserting A, $\bar{A}$, B, $\bar{B}$, C, $\bar{C}$ type layers after the $\bar{B}$ layer in the $\bar{A}\bar{B}$ unit cell. It is found that the insertions of $\bar{A}$ and $\bar{B}$ layers lead to two intrinsic fault configurations leaving only four possible extrinsic fault configurations in the $2M_1[2\bar{2}]$ structure.

Table 3 lists the fourteen unique fault configurations in the $2M_1$ structure in the Zvyagin, RTW and the $I_p^{qrs\cdots}$ notations. These are depicted in Fig. 2 by means of stacking vectors.

Possible Fault Configurations in the 3T[222] or 3T' [$\bar{2}\bar{2}\bar{2}$] Structure

The $3T$ structure can be written in two ways:

i) $\ldots A\,B\,C\,A\,B\,C\ldots = [222]\,3T$
ii) $\ldots A\,C\,B\,A\,C\,B\ldots = [\bar{2}\bar{2}\bar{2}]\,3T'$

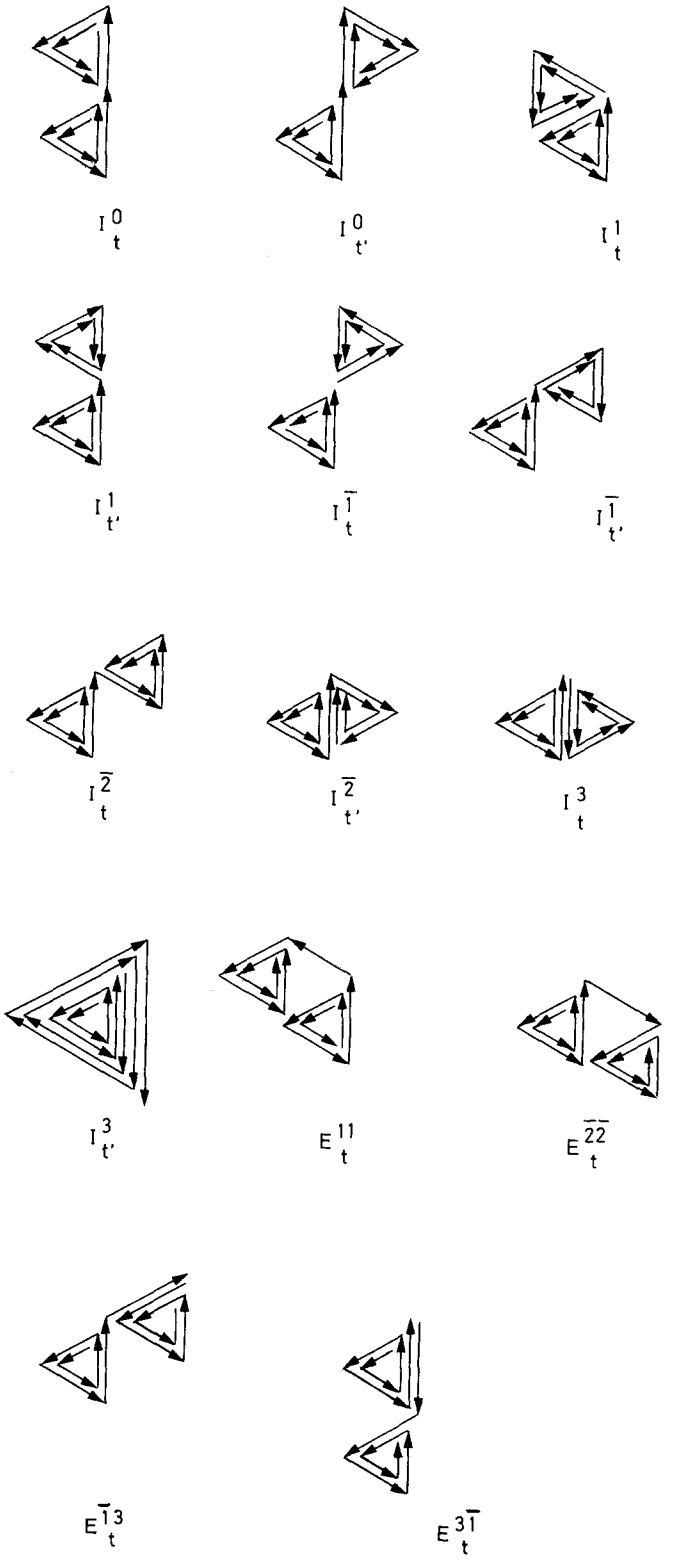

Fig. 3. Irreducible types of intrinsic and extrinsic fault configurations in the $3T$ basic matrix

These structures are enantiomorphous and cannot be distinguished by X-ray methods unless they occur in the same crystal. Thus the fault configurations in [$\bar{2}\bar{2}\bar{2}$] will be enantiomorphous with those in the [222] structure. We shall therefore deduce the possible fault configurations in the $3T$[222] (ABC) structure only. In this structure, fault configurations occuring after A, B and C layers are identical. If the intrinsic fault commences after C type layer, then the first faulted layer can be $\bar{A}$, B, $\bar{B}$, C or $\bar{C}$. Starting with each faulted layer, a fresh $3T$ sequence can be written in two different ways: one corresponding to the sequence [222] and the other corresponding to the sequence [$\bar{2}\bar{2}\bar{2}$]. Both these possibilities need to be considered in deducing the possible intrinsic fault configurations. This provides ten unique intrinsic fault configurations in the $3T$ structure.

The extrinsic fault configurations were deduced by inserting A, $\bar{A}$, B, $\bar{B}$, C, $\bar{C}$ type layers after the C type layer in the $\ldots ABC\ldots$ sequence. It is found that the insertion of A and C type layers leads to the two intrinsic fault configurations deduced earlier. We are thus left with only four unique extrinsic fault configurations in the $3T$ structure. Table 4 and Fig.3 lists and portrays respectively the fourteen unique intrinsic and extrinsic fault configurations in the $3T$ structure. To use the $I_p^{qrs\cdots}$ notation in the $3T$ structure, it is essential to specify the RTW symbol just succeeding the faulted RTW symbol(s) since the sequences on either side of the fault plane may be either identical ($3T-3T$) or different ($3T-3T'$). Therefore, we shall use either t or t' as subscripts instead of p in the I_p^{qrs} notation to distinguish the upper $3T$ and $3T'$ sequences, respectively. This nomenclature has been found to be more suitable than the one we used earlier (Baronnet et al. 1981). Accordingly, the different intrinsic fault configurations listed in Table 4 have been represented as $I_t^{qrs\cdots}$ or $I_{t'}^{qrs\cdots}$.

The Most Probable Fault Configuration

The probability of occurrence of the different fault configurations during the layer by layer growth of a basic structure will be determined by their relative stacking fault energies. Employing the notation used by Hirth and Lothe (1968) the *energy of a stacking fault* (SFE) can be expressed as:

$$\mathrm{SFE} = \sum_n \mathrm{r}_n\,\phi_n$$

where ϕ_n is the distortional energy per faulted pair of layers with n-layer separation and r_n is the number of such faulted pairs.

Unlike close-packed structures, ϕ_1 here may not always be zero and will be represented by $\phi_1\,(a_x)$ where a_x corresponds to the RTW symbols of the faulted stacking angle. The RTW symbol corresponds to the stacking angle between successive layers and therefore represents the relationship between a pair of mica unit layers with one-layer separation. If some of the RTW symbols in the fault configuration do not belong to the symbols already present in the perfect basic structure, they would contribute ϕ_1 terms towards the total SFE. Thus $\phi_1(0)$ in $1M$, $\phi_1(2)=\phi_1(\bar{2})=0$ in $2M_1$ and $3T$. The non zero $\phi_1(a_x)$ terms are: $\phi_1(1)=\phi_1(\bar{1})$, $\phi_1(2)=\phi_1(\bar{2})$, $\phi_1(3)$ in $1M$ and $\phi_1(0)$, $\phi_1(1)=\phi_1(\bar{1})$, $\phi_1(3)$ in $2M_1$ and $3T$.

To determine the terms in ϕ_2, we look at the stacking angles between layers $n-1$, n and n, $n+1$. The permissible stacking angles between layers $n-1$, n and n, $n+1$ are:

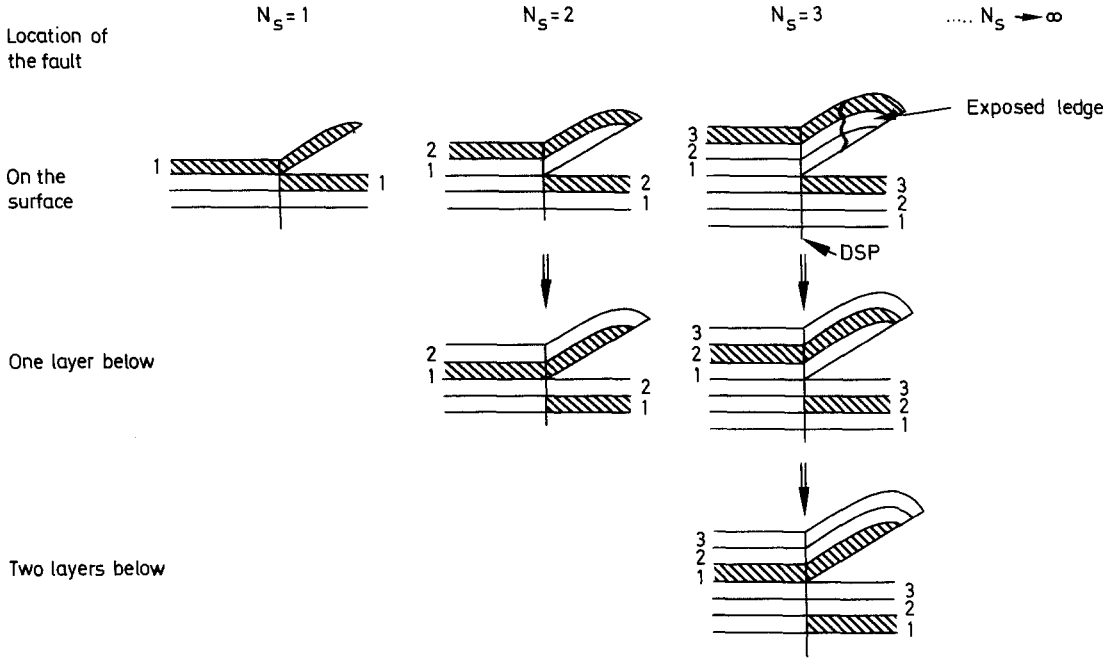

Fig. 4. Schematic representation of the method of deduction of polytype structures by spiral growth on a faulted matrix. The exposed ledge of N_s layers contains a single stacking fault, shown by the striped layers. The layer-position of the fault in the exposed ledge depends on its location from the surface of the matrix. DSP represents the *dislocation shear plane.*

0 and 0 respectively in $1M$, 2 and $\bar{2}$ or $\bar{2}$ and 2 in $2M_1$ and 2 and 2 or $\bar{2}$ and $\bar{2}$ in $3T$ implying $\phi_2(00)=0$ for $1M$, $\phi_2(2\bar{2})=\phi_2(\bar{2}2)=0$ for $2M_1$ and $\phi_2(22)=\phi_2(\bar{2}\bar{2})=0$ for $3T$. Any deviation from the permissible stacking angles between layers $n-1$, n and n, $n+1$ in the perfect structure would contribute a non-zero ϕ_2 term towards the total SFE. Since ϕ_2 will in general be much less than ϕ_1, we shall assume that the different types of faulted pairs of layers with two-layer separation have almost equal distortional energy. It should be noted that ϕ_1 and ϕ_2 have different values for different basic structures.

Following the procedure discussed above, we have estimated the SFE of different fault configurations in the $1M$, $2M_1$ and $3T$ structures up to ϕ_2 terms. These values are given in the last column of Tables 2, 3 and 4. It is evident from the tables, that the following fault configurations which are listed in order of decreasing probability of occurrence or increasing SFE values, would be more probable:

$1M: I_0^2,\ E_0^{2\bar{2}}$, |assuming that $\phi_1(2)<\phi_1(1)$ or $\phi_1(3)$|

$2M_1: I_2^2,\ I_2^{22},\ E_2^{222}$

$3T: I_t^{\bar{2}},\ I_t^{\bar{2}},\ E_t^{\bar{2}\bar{2}}$

The SFE values of all the fault configurations in the $1M$ structure contain one or more $\phi_1(a_x)$ terms. In deciding the more probable fault configurations in this structure, we have therefore used the experimental observation (Ross et al. 1966) that stacking angles of $\pm 120°$ are more common than $\pm 60°$ or $180°$ implying $\phi_1(2)<\phi_1(1)$ or $\phi_1(3)$. This holds since the (1 mod2) $\pi/3$ stacking angles distort the coordination polyhedra of alkali ions in the actual mica structure.

The Deduction of Polytype Structures

We shall now deduce all possible series of structures that can result by spiral growth round a single screw dislocation created in the $1M$, $2M_1$ and $3T$ basic matrices taking into account the possibility that stacking faults present near the surface can affect the structure of the exposed ledge. This is done by considering each of the more probable fault configurations to lie at different distances from the surface of the basic matrix at the time of the creation of the screw dislocation ledge as illustrated in Fig. 4. The periodicity of the resulting polytype structure will be determined by the number N_s of single layers present in the exposed ledge of the screw dislocation. N_s may take the following possible integral and non-integral values with respect to the repeat period of the basic structure:

$1M$: $N_s = 0$ mod 1
$2M_1$: $N_s = 0$ mod 2, and 1 mod 2
$3T$: $N_s = 0$ mod 3, 1 mod 3, and 2 mod 3.

It will be assumed that the screw dislocation ledge contains a single more probable fault configuration. The possibility

Table 5. Deduction of possible series of structures resulting from 8-layered screw dislocation ledge containing a single I_2^2 fault in the $2M_1$ matrix

S.No.	Structure of the ledge (in Zvyagin's notation)	Resulting polytype (in RTW notation)
1.	$\bar{B}\ \bar{A}\ \bar{B}\ \bar{A}\ \bar{B}\ \bar{A}\ \bar{B} \vdots \bar{C}$	$(\bar{2}2)_3(2\bar{2})$
2.	$\bar{A}\ \bar{B}\ \bar{A}\ \bar{B}\ \bar{A}\ \bar{B} \vdots \bar{C}\ \bar{B}$	$(\bar{2}2)_3(2\bar{2})$
3.	$\bar{B}\ \bar{A}\ \bar{B}\ \bar{A}\ \bar{B} \vdots \bar{C}\ \bar{B}\ \bar{C}$	$(\bar{2}2)_2(2\bar{2})_2$
4.	$\bar{A}\ \bar{B}\ \bar{A}\ \bar{B} \vdots \bar{C}\ \bar{B}\ \bar{C}\ \bar{B}$	$(\bar{2}2)_2(2\bar{2})_2$
5.	$\bar{B}\ \bar{A}\ \bar{B} \vdots \bar{C}\ \bar{B}\ \bar{C}\ \bar{B}\ \bar{C}$	$(\bar{2}2)\ (2\bar{2})_3$
6.	$\bar{A}\ \bar{B} \vdots \bar{C}\ \bar{B}\ \bar{C}\ \bar{B}\ \bar{C}\ \bar{B}$	$(\bar{2}2)\ (2\bar{2})_3$
7.	$\bar{B} \vdots \bar{C}\ \bar{B}\ \bar{C}\ \bar{B}\ \bar{C}\ \bar{B}\ \bar{C}$	$(2\bar{2})$

Note: Dotted vertical line indicates the fault plane with respect to the perfect stacking sequence on its left hand side

Table 6. Structure series resulting from screw dislocation ledges containing I_0^2 type fault in the $1M[0]$ structure

Fault type	No. of layers in the exposed ledge	Structure series	Stacking fault energy
I_0^2	$N_s=0$ mod 1	$(0)_n2(0)_m\bar{2}$	$2\phi_1(2)+4\phi_2$ $(n, m\neq 0)$ $2\phi_1(2)+3\phi_2$ (n or $m=0$) $2\phi_1(2)+2\phi_2$ $(n=m=0)$

Table 7. Structure series resulting from screw dislocation ledges containing a single more probable fault in the $2M_1[2\bar{2}]$ structure

Fault type	No. of layer in the exposed ledge	Structure series	Stacking fault energy
I_2^2	$N_s=0$ mod 2	$(\bar{2}2)_n(2\bar{2})_m$	$0\phi_1+2\phi_2$ $(n, m\neq 0)$
	$N_s=1$ mod 2	$(\bar{2}2)_n(2\bar{2})_m222$	$0\phi_1+3\phi_2$
		$(\bar{2}2)_n(2\bar{2})_m0$	$\phi_1(0)+3\phi_2$ $(n, m\neq 0)$
			$\phi_1(0)+2\phi_2$ (n or $m=0$)
I_2^{22}	$N_s=0$ mod 2	$(\bar{2}2)_n(2\bar{2})_m$	$0\phi_1+2\phi_2$ $(n, m\neq 0)$
		$(\bar{2}2)_n22(\bar{2}2)_m02$	$\phi_1(0)+4\phi_2$
		$(\bar{2}2)_n22(\bar{2}2)_m\bar{2}\bar{2}$	$0\phi_1+4\phi_2$ $(n\neq 0)$
			$0\phi_1+2\phi_2$ $(n=0)$
	$N_s=1$ mod 2	$(\bar{2}2)_n(2\bar{2})_m222$	$0\phi_1+3\phi_2$
E_2^{222}	$N_s=0$ mod 2	$(\bar{2}2)_n2\bar{2}$	$0\phi_1+2\phi_2$ $(n\neq 0)$
		$(\bar{2}2)_n22(2\bar{2})_m02$	$\phi_1(0)+4\phi_2$ ($m=0$, $n\neq 0$ or $n=m=0$)
			$\phi_1(0)+5\phi_2$ ($n=0$, $m=0$ or $n, m\neq 0$)
		$(\bar{2}2)_n22(2\bar{2})_m20$	$\phi_1(0)+5\phi_2$ ($n, m\neq 0$ or $n\neq 0$, $m=0$)
			$\phi_1(0)+4\phi_2$ ($n=0$, $m\neq 0$, or $n=m=0$)
	$N_s=1$ mod 2	$(\bar{2}2)_n222$	$0\phi_1+3\phi_2$

of a ledge containing two or more fault configurations cannot be ruled out especially in the case of screw dislocations of large Burgers vectors. Table 5 illustrates the method of deducing possible polytype structures for the case of a ledge of eight layers exposed in a $2M_1$ matrix containing a single I_2^2 type fault near its surface. It is easy to see that the resulting structures belong to the structure series $(\bar{2}2)_n(2\bar{2})_m$ where n and m are any integers 0, 1, 2, 3, etc. In a similar way, the possible series of structures that can result from screw dislocations of different Burgers vectors

Table 8. Structure series resulting from screw dislocation ledges containing a single more probable fault in the $3T[222]$ structure

Fault type	No. of layers in the exposed ledge	Structure series	Stacking fault energy
$I_{t'}^{\bar{2}}$	$N_s=0$ mod 3	$(222)_n(\bar{2}\bar{2}\bar{2})_m$	$0\phi_1+2\phi_2$ $(n, m\neq 0)$
		$(222)_n2(\bar{2}\bar{2}\bar{2})_m\bar{2}0$	$\phi_1(0)+3\phi_2$
	$N_s=1$ mod 3	$(222)_n22(\bar{2}\bar{2}\bar{2})_m\bar{2}\bar{2}$	$0\phi_1+2\phi_2$
		$(222)_n(\bar{2}\bar{2}\bar{2})_m0$	$\phi_1(0)+3\phi_2$ $(n, m\neq 0)$
			$\phi_1(0)+2\phi_2$ (n or $m=0$)
	$N_s=2$ mod 3	$(222)_n2(\bar{2}\bar{2}\bar{2})_m\bar{2}$	$0\phi+2\phi_2$
		$(222)_n22(\bar{2}\bar{2}\bar{2})_m\bar{2}\bar{2}0$	$\phi_1(0)+3\phi_2$
$I_t^{\bar{2}}$	$N_s=0$ mod 3	$(222)_n2\bar{2}(222)_m0$	$\phi_1(0)+4\phi_2$ $(m\neq 0)$
			$\phi_1(0)+3\phi_2$ $(m=0)$
		$(222)_n\bar{2}2(222)_m0$	$\phi_1(0)+4\phi_2$ $(n\neq 0)$
			$\phi_1(0)+3\phi_2$ $(n=0)$
		$(222)_n22\bar{2}(222)_m220$	$\phi_1(0)+4\phi_2$
	$N_s=1$ mod 3	$(222)_n22\bar{2}(222)_m\bar{2}$	$0\phi_1+4\phi_2$ $(m\neq 0)$
			$0\phi_1+2\phi_2$ $(m=0)$
		$(222)_n2\bar{2}(222)_m2\bar{2}$	$0\phi_1+4\phi_2$
		$(222)_n\bar{2}2(222)_m2\bar{2}$	$0\phi_1+4\phi_2$ $(n\neq 0)$
			$0\phi_1+2\phi_2$ $(n=0)$
	$N_s=2$ mod 3	$(222)_n2\bar{2}$	$0\phi_1+2\phi_2$
$E_t^{\bar{2}\bar{2}}$	$N_s=0$ mod 3	$(222)_n2\bar{2}(222)_m0$	$\phi_1(0)+4\phi_2$ $(m\neq 0)$
			$\phi_1(0)+3\phi_2$ $(m=0)$
		$(222)_n\bar{2}2(222)_m0$	$\phi_1(0)+4\phi_2$ $(n\neq 0)$
			$\phi_1(0)+3\phi_2$ $(n=0)$
		$(222)_n22\bar{2}(222)_m220$	$\phi_1(0)+4\phi_2$
	$N_s=1$ mod 3	$(222)_n0$	$\phi_1(0)+2\phi_2$ $(n\neq 0)$
	$N_s=2$ mod 3	$(222)_n0(222)_m0$	$2\phi_1(0)+4\phi_2$ $(n, m\neq 0)$
			$2\phi_1(0)+3\phi_2$ (n or $m=0$)
		$(222)_n220(222)_m20$	$2\phi_1(0)+4\phi_2$
		$(222)_n2\bar{2}$	$2\phi_2$

created in faulted $1M[0]$, $2M_1[2\bar{2}]$ and $3T[222]$ matrices were worked out. Tables 6, 7 and 8 list the results obtained from such an analysis for the $1M$, $2M_1$ and $3T$ matrices respectively.

The Most Probable Series of Structures

According to Pandey and Krishna (1975d), the relative probability of occurrence of the different structure series will be governed by (i) the energy of the fault configuration present near the surface of the matrix at the time of the creation of the screw dislocation step, (ii) the energy of the screw dislocation responsible for the generation of the structure, and (iii) the stacking fault energy of the resulting polytype. In order to obtain the most probable series of structures, it is meaningful only to compare the SFE of the different structure series that can result from a screw dislocation of the same Burgers vector (same elastic energy stored by the dislocation) created in the same basic matrix containing the most probable (i.e., the lowest energy) fault configuration. To do this we have estimated the SFE of the different series of structures listed in Tables 6, 7 and 8 up to the ϕ_2 terms. The method used for SFE estimates of polytype structures is similar to that described for isolated fault configurations except for the fact that layers within one unit cell only are considered. The SFE values, so estimated, are given in the last columns of Tables 6, 7 and 8. It should be noted that the SFE values of the different structures are usually either equal to, or greater than, the SFE of the corresponding isolated faults. This last case is due to the creation of additional stacking faults by the piling up of one unit cell over the other during the spiral growth.

Table 9 lists the most probable series of structures for different basic structures predicted on the basis of the faulted matrix model.

Table 9. The most probable series of structures resulting from theoretical screw dislocation ledges containing a single lowest energy fault configuration

No. of layers in the exposed ledge	Fault type	Structure series	Known polytypes
$N_s=0$ mod 1	I_0^2	$(0)_n2(0)_m\bar{2}$	$3Tc$, $4Tc_2$, $8Tc_2$, $9Tc$, $14Tc$, $23Tc$
$N_s=0$ mod 2	I_2^2	$(\bar{2}2)_n(2\bar{2})_m$	$8Tc_1$
$N_s=1$ mod 2	I_2^2	$(\bar{2}2)_n(2\bar{2})_m222$	$5M$
$N_s=0$ mod 3	$I_{t'}^{\bar{2}}$	$(222)_n(\bar{2}\bar{2}\bar{2})_m$	
$N_s=1$ mod 3	$I_{t'}^{\bar{2}}$	$(222)_n22(\bar{2}\bar{2}\bar{2})_m\bar{2}\bar{2}$	
$N_s=2$ mod 3	$I_{t'}^{\bar{2}}$	$(222)_n2(\bar{2}\bar{2}\bar{2})_m\bar{2}$	$5M$, $8M$, $11M$, $14M$

Table 10. List of mica polytypes with known structures

S.No.	Polytypes		
	Ramsdell notation	RTW notation	Zvyagin notation
1.	$3Tc$	$02\bar{2}$	CAC
2.	$3M$	$11\bar{2}$	$\bar{A}C\bar{B}$
3.	$4Tc_1$	0132	$C\bar{B}BC$
4.	$4Tc_2$	$(0)_2 2\bar{2}$	$(C)_2AC$
5.	$4M$	2220	$CABC$
6.	$5Tc$	$0(\bar{2}2)_2$	$(\bar{A}\bar{B})_2\bar{A}$
7.	$5M$	$(222)2\bar{2}$	$CABCA$
8.	$8Tc_1$	$(2\bar{2})_3\bar{2}2$	$(\bar{A}\bar{B})_3\bar{A}\bar{C}$
9.	$8Tc_2$	$(0)_6 2\bar{2}$	$(C)_6AC$
10.	$8Tc_3$	$(0)_3 2\bar{2}\bar{2}02$	$(C)_4ACBB$
		or $(0)_3 20\bar{2}\bar{2}2$	$(C)_4AACB$
11.	$8M$	$(222)_2 2\bar{2}$	$(CAB)_2CA$
12.	$9Tc$	$(0)_7 2\bar{2}$	$(C)_7AC$
13.	$10Tc$	$(2)_5\bar{2}2200$	$(CAB)_2ABCC$
		or $(2)_5 00222$	$(CAB)_2BBCA$
14.	$11M$	$(222)_3 2\bar{2}$	$(CAB)_3CA$
15.	$14Tc$	$(0)_{12} 2\bar{2}$	$(C)_{12}AC$
16.	$14M$	$(222)_4 2\bar{2}$	$(CAB)_4CA$
17.	$18Tc$	$(0_{n_1-1}2(0)_{n_2-1}$ $2(0)_{n_3-1}2$ with $n_3<n_1<n_2$ and $n_1+n_2+n_3\simeq 18$	
18.	$23Tc$	$(0)_{21} 2\bar{2}$	$(C)_{21}AC$

Discussion of Results

We shall now compare the observed polytype structures with the most probable series of structures predicted theoretically on the basis of the faulted matrix model. Table 10 lists the eighteen complex polytype structures that have been reported so far in the literature. A comparison of Tables 9 and 10 shows that of the eighteen known polytype structures, eleven belong to the most probable series of structures predicted theoretically on the basis of the faulted matrix model. Of the remaining seven polytype structures, $5Tc[0(\bar{2}2)_2]$ and $4M[2220]$ can result from $2M_1$ and $3T$ matrices containing I_2^0 and I_t^0 fault configurations respectively but correspond to the second most probable structure. The other five polytype structures, namely $3M[11\bar{2}]$, $4Tc[0132]$, $8Tc[(0)_3\bar{2}\bar{2}202]$, $10Tc[(2)_5\bar{2}2200]$, and $18Tc[(0)_{n_1-1}2(0)_{n_2-1}2(0)_{n_3-1}2]$, can result from singly- or multiply-faulted exposed ledges containing higher energy fault configurations. These polytypes therefore represent less probable structures which can be expected to form very rarely in nature. Thus the origin of all the known polytype structures of mica can be explained if one considers spiral growth round single screw dislocations created in a faulted matrix. It should be noted that the origin of only seven of the eighteen known polytypes (including the above $5Tc$ and $4M$) could be directly explained from a consideration of perfect basic matrices (Baronnet 1975).

On the basis of the faulted matrix model developed here to account for the growth of polytypes, it is possible to predict the most probable structure series to which a new polytype may belong, provided the structure on which it is based is known. Generally, a quick inspection of the intensity and periodicity features along hk*l* rows of reflections ($k\neq 3n$) recorded on X-ray photographs, is sufficient for the determination of this basic structure. In such cases the structure determination of polytypes, especially those with a long repeat, can be greatly simplified by theoretically predicting the more likely structures to be tried on the basis of the present, faulted-matrix model. As an example, for

the observed 23-layered polytype, there are over $3 \cdot 10^8$ possible and distinct structures if the stacking angles are restricted to 0°, +120° and −120° only – micas with so-called "ternary" structures – (Mogami et al. 1978; McLarnan 1981). However, according to the faulted-matrix model, only ten structures need to be tried if we assume for instance a $1M$ basic structure. The observed $23Tc$ (see Table 9) belongs to one of these ten more probable structures.

While predicting the most probable series of structures we have not considered an additional energy term resulting from the lattice mismatch across the shear plane of the screw dislocation (Baronnet 1980). It is however impossible to quantify this contribution since it depends on the number, nature and distribution of the stacking faults in the parent matrix as well as on the thickness of the parent platelet. Nevertheless, it is easy to realize that the presence of stacking faults may locally reestablish a good fit across the shear plane, and thereby reduce the average misfit energy as compared to its value for an identical screw dislocation in a perfect parent matrix. This is true if the dislocation pitch is a non-integral multiple of the basic structure repeat distance.

Appendix

Stacking Sequence Nomenclatures and Graphic Representation of Mica Layers

The notation proposed by Zvyagin (1962) describes the positions of successive mica layers with respect to a standard layer in C position. To a single layer n is attached a Zvyagin symbol A_n which may be either C, $\bar{B}$, $\bar{A}$, A, B or $\bar{C}$ if the rotation of any layer n with respect to the standard layer is 0°, +60°, −60°, +120°, −120° or 180°, respectively. The full sequence of a N_s-layered polytype writes as a series of N_s Zvyagin symbols between parentheses:

$$(A_1 A_2 A_3 \ldots A_n \ldots A_{N_s-1} A_{N_s}).$$

The successive symbols describe the stacking sequence from bottom to top.

The *Ross-Takeda-Wones* (RTW) rotational notation is a series of figure symbols a_n between square brackets describing each the successive stacking angles between consecutive layers n and $n+1$, from bottom to top. They are 0, 1, $\bar{1}$, 2, $\bar{2}$ or 3 and refer to 0°, +60°, −60°, +120°, −120° or 180° interlayer stacking angles, respectively. Following the RTW notation, the stacking sequence of the above N_s-layered polytype writes as:

$$[a_1 a_2 a_3 \ldots . a_n \ldots . a_{N_s-1} a_{N_s}]$$

Since the layer N_s+n must be in the same positions as layer n, the following periodicity condition must hold RTW symbols:

$$a_{N_s} + \sum_{n=1}^{N_s-1} a_n = 0 \bmod 6$$

During spiral growth, $a_1 a_2 \ldots . a_{N_s-1}$ are directly inherited from the stacking scheme in the exposed ledge of the screw dislocation, whereas a_{N_s} is due to the piling up of layer 1 over layer N_s (see Fig. 4). If a_{N_s} is a foreign symbol (in nature or location) within the basic structure, then an additive stacking fault is introduced by spiral growth itself.

The graphic representation of the stacking sequences (Smith and Yoder 1956) used in Figs. 1–3 displays the suite of stacking vectors viewed along c^x (normal to the layers), from bottom to top.

Acknowledgements. This work has been carried out as part of the existing Scientific Cooperation Programme between France and India. Financial support from the CNRS (France) and CSIR (India) to A. Baronnet and from CNRS (France) and the Laboratoire de Minéralogie Cristallographie of University of Lyon (I) to D. Pandey is gratefully acknowledged.

References

Amelinckx S (1952) La croissance hélicoïdale des cristaux de biotite. C R Acad Sci Paris 234:971–973

Amelinckx S, Dekeyser W (1953) Le polytypisme des minéraux micacés et argileux. I: Observations et interprétations. C R Congr Géol Intern Algiers 1952–18:9–22

Bailey SW (1980) Structures of layer silicates. In: Brindley GW, Brown G (eds) Crystal Structures of clay minerals and their X-ray identification, Mineralogical Society London 1980, pp 1–124

Bailey SW, Christie OHJ (1978) Three-layer monoclinic lepidolite from Tørdal, Norway. Am Mineral 63:203–204

Baronnet A (1972) Growth mechanisms and polytypism in synthetic hydroxyl-bearing phlogopite. Am Mineral 57:1272–1293

Baronnet A (1975) Growth spirals and complex polytypism in micas. I: Polytypic structure generation. Acta Crystallogr A31:345–355

Baronnet A (1976) Polytypisme et polymorphisme dans les micas: Contribution à l'étude du rôle de la croissance cristalline. Dr Es Sci Thesis, Marseilles

Baronnet A (1980) Polytypism in micas: A survey with emphasis on the crystal growth aspect. Curr Top Mat Sci 5:447–548

Baronnet A, Amouric M, Chabot B (1976) Mécanismes de croissance, polytypisme et polymorphisme de la muscovite hydroxylée synthétique. J Cryst Growth 32:37–59

Baronnet A, Pandey D, Krishna P (1981) Application of the faulted matrix model to the growth of polytype structures in mica. J Cryst Growth 52:963–968

Beugnies A, Godfriaux I, Robaszynski F (1969) Contribution à l'étude des phengites. Bull Soc Belge Geol Paentol Hydrol 77:95–146

Blasi A, Blasi de Pol C (1973) $2M_1$ e $3T$ polymorfi delle miche diottaedriche coesistenti nei graniti del Massiccio dell'Argentera (Alpi Marittime). Atti Accad Naz Lincei 54:528–545

Cerny P, Rieder M, Pondrova P (1970) Three polytypes of lepidolite from Czechoslovakia. Lithos 3:319–325

Chatterjee ND (1970) Synthesis and upper stability of paragonite. Contrib Mineral Petrol 27:244–257

Chatterjee ND (1971) Preliminary results on the synthesis and upper stability limit of margarite. Naturwissenschaften 58:147

Crowley MS, Roy R (1964) Crystalline solubility in the muscovite and phlogopite groups. Am Mineral 49:348–362

Deer WA, Howie RA, Zussman J (1965) Rock-forming minerals, vol 3: Sheet silicates. Longmans, London

Dunoyer de Segonzac G, Hickel D (1972) Cristallochimie des phengites dans les quartzites micacés métamorphiques du Permo-Trias des Alpes Piémontaises. Sci Geol Bull Strasbourg 25:201–229

Ernst WG (1963) Significance of phengitic micas from low-grade schists. Am Mineral 48:1357–1373

Eugster HP, Yoder HS (1954) Paragonite. Carnegie Inst Wash Yearb 53:111–114

Fiorentini Potenza M, Morelli G (1968) Le paragenesi delle metamorfiti a fengite $3T$ e muscovite $2M_1$ in Val Chiusella – Zona Sesia – Lanzo. Atti Soc Ital Sci Nat Mus Civ Stor Nat Milano 107:5–36

Foster MD (1960) Interpretation of the composition of lithium micas. US Geol Surv Prof Pap 354E:115–146

Frank FC (1951a) The growth of carborundum: Dislocations and polytypism. Philos Mag 42:1014–1021
Frank FC (1951b) Crystal dislocations – elementary concepts and definitions. Philos Mag 42:809–819
Guven N (1971) Structural factors controlling stacking sequences in dioctahedral micas. Clays Clay Miner 134:159–165
Harder H (1956) Untersuchungen an Paragoniten und an natriumhaltigen Muskoviten. Heidelb Beitr Mineral Petrogr 5:227–271
Hewitt DA, Wones DR (1975) Physical properties of some synthetic Fe–Mg–Al trioctahedral biotites. Am Mineral 60:854–862
Hirth JP, Lothe J (1968) Theory of dislocations. Mc Graw-Hill, New York
Koval'PV, Bazarova SB, Kashagev AA (1975) Polytypism of muscovite biotite and lithium mica types as a function of composition and genesis. Dokl Akad Nauk SSSR 225:125–128
Levinson AA (1953) Studies in the mica group; relationship between polymorphism and composition in the muscovite-lepidolite series. Am Mineral 38:88–107
McLarnan TJ (1981) The numbers of polytypes in sheet silicates. Z Kristallogr 155:247–268
Mogami K, Nomura K, Miyamoto M, Takeda H, Sadanaga R (1978) On the number of distinct polytypes of micas and SiC with a prime layer-number. Can Mineral 16:427–435
Munoz JL (1968) Physical properties of synthetic lepidolites. Am Mineral 53:1490–1512
Olesch M (1975) Synthesis and solid solubility of trioctahedral brittle micas in the system $CaO-MgO-Al_2O_3-SiO_2-H_2O$. Am Mineral 60:188–199
Pandey D, Krishna P (1975a) Influence of stacking faults on the growth of polytype structures. I – Cadmium iodide polytypes. Philos Mag 31:1113–1132
Pandey D, Krishna P (1975b) Influence of stacking faults on the growth of polytype structures. II – Silicon carbide polytypes. Philos Mag 31:1133–1148
Pandey D, Krishna P (1975c) A faulted matrix model for the spiral growth of polytype structures. Phys Lett 51A:209–210
Pandey D, Krishna P (1975d) On the spiral growth of polytype structures in SiC from a faulted matrix. I: Polytypes based on the 6*H* structure. Mater Sci Eng 20:234–249
Pandey D, Krishna P (1976) On the spiral growth of polytype structures in SiC from a faulted matrix. II: Polytypes based on the 4*H* and 15*R* structures. Mater Sci Eng 26:53–63
Rieder M (1970) Lithium-iron micas from the Krusné Hory Mountains (Erzgebirge) : Twins, epitactic overgrowths and polytypes. Z Kristallogr 132:161–184
Rieder M (1971) Stability and physical properties of synthetic lithium – iron micas. Am Mineral 56:256–280
Ross M, Takeda H, Wones DR (1966) Mica polytypes: Systematic description and identification. Science 151:191–193
Smith JV, Yoder HS (1956) Experimental and theoretical studies of the mica polymorphs. Mineral Mag 31:209–235
Takeda H (1967) Determination of the layer stacking sequence of a new complex mica polytype: A 4-layer lithium fluorophlogopite. Acta Crystallogr 22:845–853
Takeuchi Y, Haga N (1971) Structural transformations of trioctahedral sheet silicates. Slip mechanisms of octahedral sheets and polytypic changes in micas. J Mineral Soc Japan Spec Pap 1:74–87
Velde B (1965a) Experimental determination of muscovite polymorph stabilities. Am Mineral 50:436–449
Velde B (1965b) Phengite micas: Synthesis, stability and natural occurrence. Am J Sci 263:886–913
Velde B (1970) Les éclogites de la région nantaise (de Campbon au Cellier, Loire-Atlantique). Bull Soc Fr Mineral Cristallogr 93:370–385
Velde B (1971) The stability and natural occurrence of margarite. Mineral Mag 38:317–323
Wones DR (1963) Physical properties of synthetic biotites on the join phlogopite-annite. Am Mineral 48:1300–1321
Yoder HS (1959) Experimental studies on micas: A synthesis. Proc Sixth Nation Conf Clays Clay Miner. Pergamon Press, London, pp 42–60
Yoder HS, Eugster HP (1954) Phlogopite synthesis and stability range. Geochim Cosmochim Acta 6:157–185
Yoder HS, Eugster HP (1955) Synthetic and natural muscovites. Geochim Cosmochim Acta 8:225–280
Zhoukhlistov AP, Zvyagin BB, Soboleva SV, Fedotov AF (1973) The crystal structure of the dioctahedral mica $2M_2$ determined by high voltage electron diffraction. Clays Clay Miner 21:465–470
Zvyagin BB (1962) A theory of polymorphism in micas. Sov Phys Crystallogr 6:571–580

Received December 10, 1981